Low-temperature H2 sensing in self-assembled organotin thin films

Laetitia Renard, Hicham Elhamzaoui, Bernard Jousseaume, Thierry Toupance, Guillaume Laurent, François Ribot, Hassan Saadaoui, Joachim Brötz, Hartmut Fuess, Ralf Riedel, et al.

Low-temperature H_2 sensing in self-assembled organotin thin films

Laetitia Renard,[a] Hicham Elhamzaoui,[a] Bernard Jousseaume,[a] Thierry Toupance,*[a] Guillaume Laurent,[b] François Ribot,[b] Hassan Saadaoui,[c] Joachim Brötz,[d] Hartmut Fuess,[d] Ralf Riedel,[d] and Aleksander Gurlo.*[d]

Received 1st October 2010, Accepted 11th November 2010

Self-assembled nanoporous tin-based hybrid thin films prepared by the sol-gel method from organically-bridged ditin hexaalkynides detect hydrogen gas from 50 to 200°C at the 200-10000 ppm level. This finding opens a fully new class of gas-sensing materials as well as a new opportunity to integrate organic functionality in gas sensing metal oxides.

Organic-inorganic hybrid materials combine on the nanometre scale active inorganic and organic components providing in this way novel functionalities. Thus, in oxide-based hybrids, the synergy between the outstanding chemical and electronic properties of metal oxides with the functional flexibility offered by an organic component allows for sophisticated applications in various emerging fields including nanooptics, nanoelectronics, and energy storage or conversion.[1] Tailored-made SiO_2-based hybrids, which have been obtained by different routes including conventional sol-gel route, self-assembly procedures, nanobuilding blocks approaches, post-functionalization routes and integrative chemistry methods, are the best known and most studied organic-inorganic materials.[1a] For instance, the microstructure, texture and morphology of silica-based class II hybrids, i.e. non-crystalline materials with strong covalent bonds between inorganic and organic parts, can be controlled (in powders[2] and films[3]) via sol-gel routes utilising bridged silsesquioxanes X_3Si-R-SiX_3 (X = OR^1, Cl)[4] by appropriate tuning of the hydrolysis conditions (with or without an organic template)[5] or of the nature of the organic spacer R.[6]

Gas detection is one of the most promising applications of such hybrid organic-inorganic materials since organic groups could provide selectivity in determination of target gases. Gas sensors have gained particular attention in recent years since they are increasingly relevant for mass-market applications. Among them, chemiresistors, i.e. sensors which inform about the composition of their ambient atmosphere through changes in the conductivity/conductance of sensing materials, are the most investigated group of sensors. Despite the application of silica-based hybrids in optical sensors, these materials are not appropriate for chemiresistors due to the pure electronic conductivity of SiO_2. The most commonly used and the best-understood prototype material in the commercial chemiresistors as well as in the basic studies on gas sensing mechanism of metal oxides is tin dioxide (SnO_2).[7] However, the gas sensing properties of the hybrid non-crystalline tin-based materials have not been studied so far. Only a few studies about gas sensing properties of crystalline SnO_2 functionalized with organic molecules are known.[8]

Here we report on gas-sensing activity of self-assembled organotin thin films with alkylene and arylalkylene linkers synthesized from alkylene- and arylalkylene-bridged ditin hexaalkynides **1** (X_3Sn-R-SnX_3, where X = -C≡C-CH_3 and R = -$(CH_2)_{10}$- **1a** or -CH_2-$(C_6H_4)_2$-CH_2- **1b**). Owing to the stability of the tin-carbon bonds under conventional sol-gel hydrolytic conditions, original hydrolysable organotins for sol-gel chemistry and chemical modification of oxide surfaces have been designed.[9] Precursors **1** were thus described to widen the scope of the accessible class II hybrid materials,[10] and led to tin-based hybrid powders by the sol-gel process.[11]

The hybrid films were processed by spin-coating from a sol containing water (0.21 g, 11 mmoles), HCL 1N (0.021 g), precursor **1** (0.15 mmoles) and THF (4 g) and were then annealed at 120°C. The complete hydrolysis at 120°C required 1 and 4h for **1a** and **1b**, respectively, according to FTIR spectroscopy. Regardless of the precursor nature, the resonances expected for the organic spacer were observed in the solid state CP-MAS ^{13}C NMR spectra of the hybrid materials indicating that the spacer was incorporated in the film. For the sample including the decylene spacer, the ^{119}Sn isotropic chemical shifts around – 280 and – 460 ppm detected in the solid state CP-MAS ^{119}Sn NMR spectra can be assigned to five- and six-coordinate organotin sites, respectively, according to the previously reported ^{119}Sn shifts for oxo-hydroxo organotin species such as BuSnO(OH)[12] or $\{(RSn)_{12}(\mu_3\text{-}O)_{14}(\mu_2\text{-}OH)_6\}X_2$ clusters.[13] Both chemical shifts and chemical shift anisotropies determined by modeling the experimental spectra were also close to those found for the $\{(RSn)_{12}(\mu_3\text{-}O)_{14}(\mu_2\text{-}OH)_6\}X_2$ clusters. Similar conclusions can be drawn for the arylalkylene spacer, which – due to the electron withdrawing effect of this linker – shield the ^{119}Sn resonances (δ at ca. -325, -510, -590 and -640 ppm), confirming not only the hybrid structure of the films but also the electronic interaction between the organic linker and the SnO_x network (Fig. S1 & 2, ESI). Contact angle measurements confirmed the formation of hybrid layers (Table S1, ESI). For both linkers, the total surface energy was found to be around 27-33 mJ m^{-2} which falls within the range of that described for silsesquioxane-based polymer nanocomposites.[14] Moreover, water contact angle values confirmed the hydrophobicity of hybrid films, those processed from **1b** being slightly more hydrophobic.

AFM images of the films prepared from **1a** and **1b** revealed a relatively smooth surface (mean square roughness rms around 4.0 nm) made of a network of aggregated spherical"pseudoparticles" (Fig. 1A). Regardless of the spacer nature, the film thickness was estimated to be in the range 80-100 nm. The HRSEM images showed a relatively dense layer

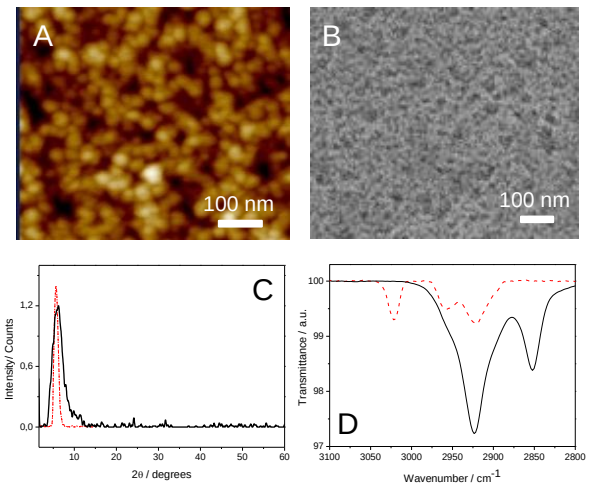

Fig. 1 (A) and (B) AFM and HR-SEM images of a film prepared from **1a**. (C) Grazing XRD patterns of the hybrids prepared from **1a** (black) and **1b** (red). (D) FTIR spectra (CH stretching vibration region) of the hybrid films prepared from **1a** (black) and **1b** (red).

with a "worm-hole"-like porous structure typical of nanoporous sol-gel materials (Fig. 1B). The GIXRD patterns showed diffraction features at ca. 2θ = 5.9° for **1a** and at 5.7° for **1b** that corresponds to interplanar spacings of about 1.5 and 1.6 nm, respectively (Fig. 1C). These values are in good agreement with those deduced from the tin-tin distance estimated from the structure of precursors **1**. Such diffraction lines account for the formation of SnO_x walls separated by organic bridges as previously found for bulk materials.[11] Furthermore, the nanostructuration of the organic linker were assessed by FTIR studies (Fig. 1D). Thus the FTIR spectrum of the alkylene-based hybrid films showed two resonances at c.a. 2920-2923 and 2850-2852 cm^{-1} that can be assigned to the asymmetric and symmetric CH_2 stretching modes. Their wave-numbers, allowing for the qualitative measurements of conformational order changes, are lower than those observed for disordered liquid alkanes[15] and are close to those reported around 2918 and 2850 cm^{-1} for crystalline-like packing of alkyl chains in self- assembled monolayers.[16] This suggests that the alkylene spacer retains a close-packed ordered assembly with few chain conformation defects. As a result, the interaction between the hydrophobic linkers seems to be favoured in the thin films that confirmed the formation of self-assembled alkylene spacer layers within the hybrid films.

Structural and morphological characterizations of hybrid organotin thin films point at (i) absence of crystalline SnO_2, (ii) "pseudoparticulate" porous morphology, and (iii) short-range hierarchical order in organic-inorganic pseudoparticles containing SnO_x networks (Fig. 2). Moreover, the comparison of the FTIR spectra of the hybrid films before and after the sensor tests clearly indicates that the films do not change their structure in the course of the gas sensing characterization (Fig. S3, ESI). On the basis of the TGA analyses, the hybrid materials are thermally stable up to 250°C, no mass loss being detected after annealing in N_2 at 200°C for several hours (Fig. S5, ESI). Accordingly, the gas-sensing properties of these hybrid materials hereafter described have to be understood in the light of these structural peculiarities.

The first finding of the gas sensing measurements (Fig. 3), i.e. dc conductance changes in dependence on gas concentration, is

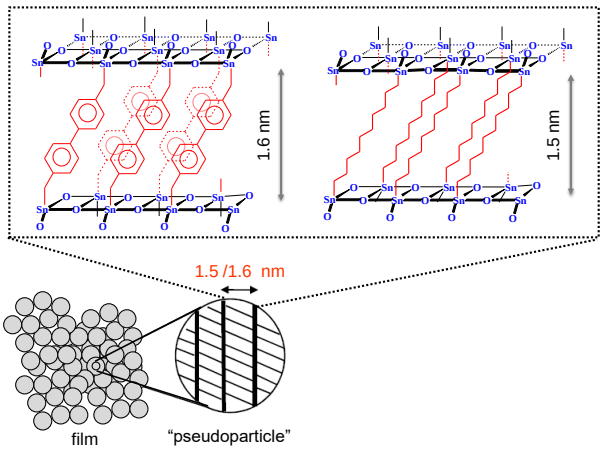

Fig. 2 Schematic representation of the hybrid structure: "pseudoparticulate" porous morphology with short-range hierarchical order in organic-inorganic pseudo-particles containing SnO_x networks.

the n-type conductivity of hybrid films. The latter show a decrease in the resistance upon exposure to H_2 (Fig. 3A, B and D) and an increase in the resistance upon exposure to O_2 (Fig. 3C). The second remarkable observation is that the hybrid films are active in gas detection possessing a near room-temperature gas sensitivity to H_2. Thirdly, the hybrid films have significantly higher responses to H_2 and O_2 at 200°C if compared with those at room temperature. At 200°C, in pure N_2, the resistance of both samples before passing of H_2 was around 10-20 kOhm, and dropped to ≈ 3-4 kOhm at 1 vol% H_2. In 1 vol% O_2/N_2, the resistance of both is higher than that in N_2 (≈ 70 kOhm); it decreases by a factor of about 10, while the samples were exposed to 1 vol% H_2. The next noticeable feature of the hybrid materials is their relative fast response to H_2 and recovery after exposure to H_2. The comparison of the initial sample resistance and the final resistance after all sensor tests shows that at 200°C all the interactions between the sensing layer and the target gases are fully reversible, even in the absence of O_2. For example, at 200°C, for the H_2 detection in 1 vol% O_2/N_2 atmosphere, the baseline resistance of the hybrids reached the initial value in less than one hour. The recovery of the baseline resistance is of crucial importance for any prospective gas sensing material.

All these observations are very surprising because – as shown above – the hybrid films do not have crystalline SnO_2 structure which is thought to be responsible for gas sensing activity in SnO_2-chemiresistors. As known, in chemiresistors based on semiconducting metal oxides the chemisorption of gas molecules results in surface charging that modifies the potential energy distribution and, by that, the effective carrier concentration near the surface. For example, the effect of O_2 adsorption is a negative charge at the surface and an increase in the band bending and work function. For an n-type semiconductor this results in the creation of a depletion layer and a decrease in surface conductivity. For O_2, the opposite effects are expected.

These results show significant differences between hybrid organic-inorganic films and SnO_2 powders in terms of both possible sensing mechanism and the sensor response. The first difference is the activity of hybrid materials at near-room temperature; the SnO_2 powder does not show any activity in H_2 detection in same conditions (at ~ 40°C).[17] The second difference

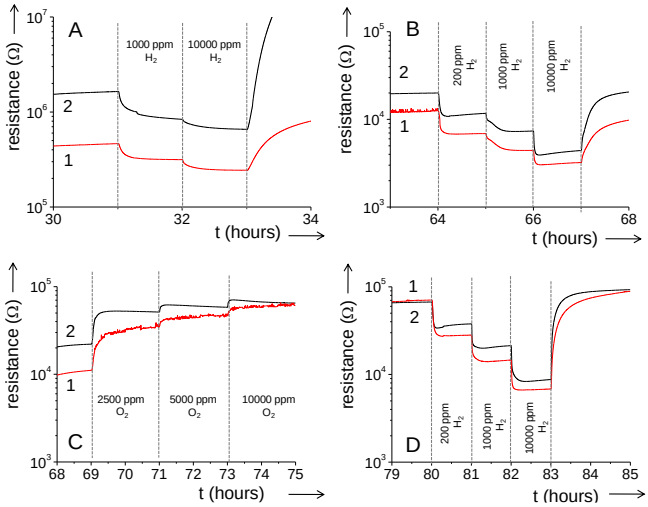

Fig. 3 Gas sensing tests. Transient response of hybrid materials at 50°C (A) and 200°C (B-D) to hydrogen (A, B, D) and oxygen (C) in nitrogen (B, C) and 1 vol% O_2/N_2 (A, D) atmospheres. Hybrid films were fabricated from **1a** (2, black) and **1b** (1, red) precursor.

with typical SnO_2 materials is the higher H_2 response in the presence of O_2 if compared to that in the oxygen-free atmosphere (at 200°C). The last one is the mechanism of H_2 detection.[17b]

The question arises about the role of the organic spacer in gas sensing activity in tin-based hybrid materials. According to the results of the dc conductance measurements the organic spacers contribute in an indirect way to the conduction as well as to the sensing mechanism of organized hybrid films. The small difference is most probably the amorphous inorganic SnO_x network. Accordingly, the sensing properties of hybrid ordered amorphous organotin films could be understood within the framework of the Davis-Mott model of electrical conductivity in ordered non-crystalline systems.[18] The main features of this model for the band structure of amorphous semiconductors are the existence of narrow tails of localized states at the extremities of the valence and conduction bands as well as a band of localized levels near the middle of the gap. The gap states in the hybrid ordered amorphous organotin films could be associated with organic spacers that electronically interact with SnO_x layers as confirmed by shielding effects observed in the NMR spectra.

In conclusion, we have shown three novel effects not known so far: (i) self-organisation in thin organotin films, (ii) their nanoporous structure and (iii) gas sensing activity of such self-organised hybrid materials. These findings have far-reaching consequences for gas sensing research since it opens a fully new class of gas-sensing materials as well as a new possibility to integrate organic functionality in gas sensing metal oxides. Further understanding of our observations for organotin films, both experimentally and theoretically, is expected to provide new insight into mechanism of gas sensing and possibly open new opportunities for tailoring the materials' properties.

We thank Mrs O. Babot and E. Sellier for their precious assistance for TGA and HR-SEM measurements. This work was carried out within the framework of the European Multifunctional Material Institute and was supported by the MENRT, the CNRS, the Aquitaine Region (Contract no. 09002556) and the European Community (FAME Network of Excellence).

Notes and references

[a] *University of Bordeaux, ISM UMR 5255 CNRS Groupe Matériaux, 33405 Talence Cédex, France. E-mail: t.toupance@ism.u-bordeaux1.fr*
[b] *LCMCP, UMR 7574 CNRS, Collège de France,, 75231 Paris Cédex 05, France.*
[c] *CRPP, UPR8641 CNRS, 33600 Pessac, France.*
[d] *Fachbereich Material- und Geowissenschaften, Technische Universitaet Darmstadt, 64287 Darmstadt, Germany. E-mail: gurlo@materials.tu-darmstadt.de*

† Electronic Supplementary Information (ESI) available: Experimental details, CP-MAS ^{119}Sn NMR spectra, surface energy data, FTIR spectra after gas sensing studies and TGA curves. DOI: 10.1039/b000000x/

1 (a) *Functional Hybrid Materials*, P. Gomez-Romero and C. Sanchez Eds, Wiley-VCH, Weinheim, 2003. (b) C. Sanchez, B. Julián, P. Belleville, M. Popall, *J. Mater. Chem.*, 2005, **15**, 3559. (c) *Hybrid Materials*, G. Kickelbick Ed., Wiley-VCH, Weinheim, 2007.

2 (a) T. Asefa, M. J. MacLachlan, N. Coombs, G. A. Ozin, *Nature*, 1999, **402**, 867; (b) S. Inagaki, S. Guan, Y. Fukushima, T. Ohsuna, O. Terasaki, *J. Am. Chem. Soc.*, 1999, **121**, 9611; (c) B. J. Melde, B. Hollande, C. F. Blanford, A. Stein, *Chem. Mater.*, 1999, **11**, 3302.

3 C. Sanchez, C. Boissière, D. Grosso, C. Laberty, L. Nicole, *Chem. Mater.*, 2008, **20**, 682.

4 (a) D. A. Loy, K. J. Shea, *Chem. Rev.*, 1995, **95**, 1431; (b) B. Boury, R. J. P. Corriu, *Chem. Commun.*, 2002, 795.

5 (a) B. Boury, F. Ben, R. J. P. Corriu, *Angew. Chem. Int. Ed* , 2001, **40**, 2853; (b) M. P. Kapoor, Q. Yang, S. Inagaki, *J. Am. Chem. Soc* , 2002, **124,** 15176; (c) B. Hatton, K. Landskron, W. Whitnall, D. Perovic, G. A. Ozin, *Acc. Chem. Res.*, 2005, **38**, 305.

6 J. J. E. Moreau, L. Vellutini, M. Wong Chi Man, C. Bied, *J. Am. Chem. Soc.*, 2001, **123**, 1509.

7 (a) N. Barsan, M. Schweizer-Berberich, W. Göpel, J. Fresenius, *Anal. Chem.*, 1999, **365**, 287; (b) T. Sahm, A. Gurlo, N. Barsan, U. Weimar, L. Madler, *Thin Solid Film* , 2005, **490**, 43; (c) L. Madler, T. Sahm, A. Gurlo, J. D. Grunwaldt, N. Barsan, U. Weimar, S. E. Pratsinis, *J. Nanopart. Res.* , 2006, **8**, 783; (d) M. Graf, A. Gurlo, N. Barsan, U. Weimar, A. Hierlemann, *J. Nanopart. Res* , 2006, **8**, 823; (e) F. Rock, A. Gurlo, U. Weimar, *Anal. Chem* , 2005, **77**, 2762.

8 (a) I. Matsubara, K. Hosono, N. Murayama, W. Shin, N. Izu, *Sensor Actuat B-Chem* , 2005, **108**, 143; (b) J. Zhang, S. R. Wang, M. J. Xu, Y. Wang, H. J. Xia, S. M. Zhang, X. Z. Guo, S. H. Wu, *J. Phys. Chem. C* , 2009, **113**, 1662.

9 (a) S. Boutet, B. Jousseaume, T. Toupance, M. Biesemans, R. Willem, C. Labrugère, L. Delattre, *Chem. Mater.*, 2005, **17**, 1803; (b) G. Vilaça, B. Jousseaume, C. Mahieux, T. Toupance, C. Belin, H. Cachet, M-C. Bernard, V. Vivier, *Adv. Mater.*, 2006, **18**, 1073.

10 B. Jousseaume, H. Riague, T. Toupance, M. Lahcini, P. Mountford, B. R. Tyrrell, *Organometallics*, 2002, **21**, 4590.

11 (a) H. El Hamzaoui, B. Jousseaume, H. Riague, T. Toupance, P. Dieudonné, C. Zakri, M. Maugey, H. Allouchi, *J. Am. Chem. Soc.*, 2004, **126**, 8130; (b) H. El Hamzaoui, T. Toupance, M. Maugey, C. Zakri, B. Jousseaume, *Langmuir*, 2007, **23**, 785. (c) H. El Hamzaoui, B. Jousseaume, T. Toupance, C. Zakri, *Dalton Trans.*, 2009, **126**, 4429.

12 F. Ribot, C. Eychenne-Baron, F. Fayon, D. Massiot, B. Bresson, *Main Group Met. Chem* , 2002, **25**, 115.

13 (a) F. Banse, F. Ribot, P. Tolédano, J. Maquet, C. Sanchez, *Inorg. Chem.*, 1995, **34**, 6371; (b) C. Eychenne-Baron, F. Ribot, N. Steunou, C. Sanchez, F. Fayon, M. Biesemans, J. C. Martins, R. Willem, *Organometallics*, 2000, **19**, 1940.

14 (a) S. Turri, M. Levi, *Macromol. Rapid Commun.*, 2005, **26**, 1233; (b) N. Hosaka, N. Torikai, H. Otsuka, A. Takahara, *Langmuir*, 2007, **23**, 902.

15 R. G. Snyder, H. L. Strauss, C. A. Elliger, *J. Phys. Chem.*, 1982, **86**, 5145.

16 A. Baptiste, A. Gibaud, J. F. Bardeau, K. Wen, R. Maoz, J. Sagiv, B. M. Ocko, *Langmuir*, 2002, **18**, 3916.

17 (a) Y. Shen, T. Yamazaki, Z. F. Liu, D. Meng, T. Kikuta, *J. Alloy Compd.*, 2009, **488**, L21; (b) G. Tournier, C. Pijolat, *Sensor Actuat B-Chem.*, 1999, **61**, 43.

18 N. Mott, *Conduction in Non-Crystalline Materials*, Clarendon Press, Oxfrod, 1987.

Supplementary Material (ESI) for Chemical Communications

Electronic Supplementary Information

Low-temperature H_2 sensing in self-assembled organotin thin films

Laetitia Renard,[a] Hicham Elhamzaoui,[a] Bernard Jousseaume,[a] Thierry Toupance,*[a] Guillaume Laurent,[b] François Ribot,[b] Hassan Saadaoui,[c] Joachim Brötz,[d] Hartmut Fuess,[d] Ralf Riedel,[d] and Aleksander Gurlo.*[d]

[a] *University of Bordeaux, ISM UMR 5255 CNRS, Groupe Matériaux, 33405 Talence Cédex, France. E-mail: t.toupance@ism.u-bordeaux1.fr*

[b] *UPMC Univ Paris 6, CMCP, UMR 7574 CNRS, Collège de France, 75231 Paris Cedex 05, France.*

[c] *CRPP, UPR 8641 CNRS, 33600 Pessac, France.*

[d] *Fachbereich Material- und Geowissenschaften, Technische Universitaet Darmstadt, 64287 Darmstadt, Germany. E-mail: gurlo@materials.tu-darmstadt.de*

Synthesis of the organotin precursor

The molecular formula of precursors **1** are shown in Scheme 1. 1,4-bis(triprop-1-ynylstannylmethyl)benzene **1b** was synthesized as previously reported.[1] All reactions were carried out under a nitrogen atmosphere. Toluene was distilled from sodium benzophenone ketyl prior to use. ^{1}H and $^{13}C\{^{1}H\}$ NMR spectra were recorded on a Bruker DPX-200 or DPX-300 spectrometer in $CDCl_3$ (δ given in ppm relative to tetramethylsilane). MALDI-MS spectra were carried out by the CESAMO (Bordeaux, France) on a Voyager mass spectrometer (Applied Biosystems) equipped with a pulse N2 laser (337 nm) and a time-delayed extracted ion source. Spectra were recorded in the positive-ion mode using the reflextron and with an accelerating voltage of 20 kV.

1,10-Bis(tripropy-1-ynyltin)decane 1a

A 2.5M solution of BuLi (4.79 mL, 11.98 mmol) was added to a solution of propyne (0.77 mL, 13.69 mmol) in toluene (10 mL) in a 100-mL 3-necked flask at –78 °C. After stirring for 15 min, a solution 1,10-Bis(trichlorotin)decane[1] (1 g, 1.71 mmol) in 20 mL of toluene was added at –78 °C. After stirring for 15 h at 70 °C, the suspension was filtered over dry $MgSO_4$, the solvent was evaporated under vacuum to give **1a** as a white solid. Yield: 95 %. ^{1}H NMR: δ 1.27 (m, 20H), 1.91 (s, 18H). ^{13}C NMR: δ 5.3 (CH_2-Sn), 15.4 (CH_3), 25.8, 29.2, 29.6, 33.2(CH_2-CH_2-Sn), 76.8 (-C≡C-Sn), 107.8 (-C≡C-Sn). ^{119}Sn NMR: δ –251.8. HRMS-MALDI: Found (calcd) $[M+Na]^+$ 637.0899 (637.0922).

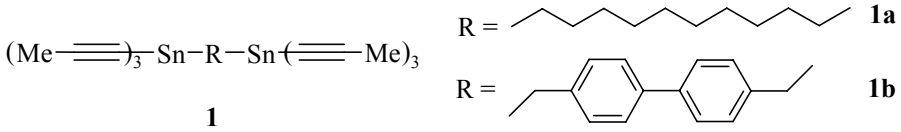

1 **1a** **1b**

Scheme S1. Precursor molecules used to prepare the hybrid thin films

(1) B. Jousseaume, H. Riague, T. Toupance, M. Lahcini, P. Mountford, B.R. Tyrrell, *Organometallics,* 2002, **21**, 4590.

Solid state CP-MAS ^{13}C and ^{119}Sn NMR studies

^{13}C and ^{119}Sn CP-MAS NMR measurement were performed on a Bruker Avance 300 spectrometer (300.29 MHz for ^{1}H, 75.52 MHz for ^{13}C and 111.92 MHz for ^{119}Sn) using a 4 mm locked Bruker probe. For both nuclei the contact time is 1 ms. ^{13}C chemical shifts are referenced towards external tetramethylsilane (TMS). ^{119}Sn chemical shifts are referenced towards tetramethyltin (TMT), using tetracyclohexyltin ($\delta = -97.35$ ppm) as a secondary external reference.[2] For ^{119}Sn, two MAS speed (14 and 11.5 kHz) were used to locate the isotropic chemical shifts.

The ^{119}Sn NMR spectra were analyzed with Dmfit,[3] and the ^{119}Sn shielding tensors extracted using the Herzfeld and Berger approach.[4] They are reported as the isotropic chemical shift ($\delta_{iso} = -\sigma_{iso}$), the anisotropy ($\zeta = \sigma_{33} - \sigma_{iso}$), and the asymmetry ($\eta = |\sigma_{22} - \sigma_{11}| / |\sigma_{33} - \sigma_{iso}|$), σ_{11}, σ_{22}, and σ_{33} being the three components of the shielding tensor expressed in its principal axis system with the following convention: $|\sigma_{33} - \sigma_{iso}| > |\sigma_{11} - \sigma_{iso}| > |\sigma_{22} - \sigma_{iso}|$.

Hybrid material from precursor **1a**.

^{13}C CP-MAS NMR: δ_{iso} (ppm) 31.0, 26.5.

^{119}Sn CP-MAS NMR: δ_{iso} (ppm) [ζ (ppm) & η] – 285 [400 & 0.0], – 458 [325 & 0.0], – 470 [312 & 0.35].

Hybrid material from precursor **1b**.

^{13}C CP-MAS NMR: δ_{iso} (ppm) 138.0, 128.9, 30.0.

^{119}Sn CP-MAS NMR: δ_{iso} (ppm) – 385, – 507, – 592, – 640.[5]

(2) H. Reuter, A. Sebald, *Z. Naturforsch,* 1992, **48B**, 195.
(3) D. Massiot, F. Fayon, M. Capron, I. King, S. Le Calvé, B. Alonso, J.-O. Durand, B. Bujoli, Z. Gan, G. Hoatson, *Magn. Res. Chem.,* 2002, **40**, 70.
(4) J. Herzfeld, A. E. Berger, *J. Chem. Phys.* 1980, **73**, 6021.
(5) Extraction of the ^{119}Sn shielding tensors was not possible. Only the isotropic chemical shifts were obtained.

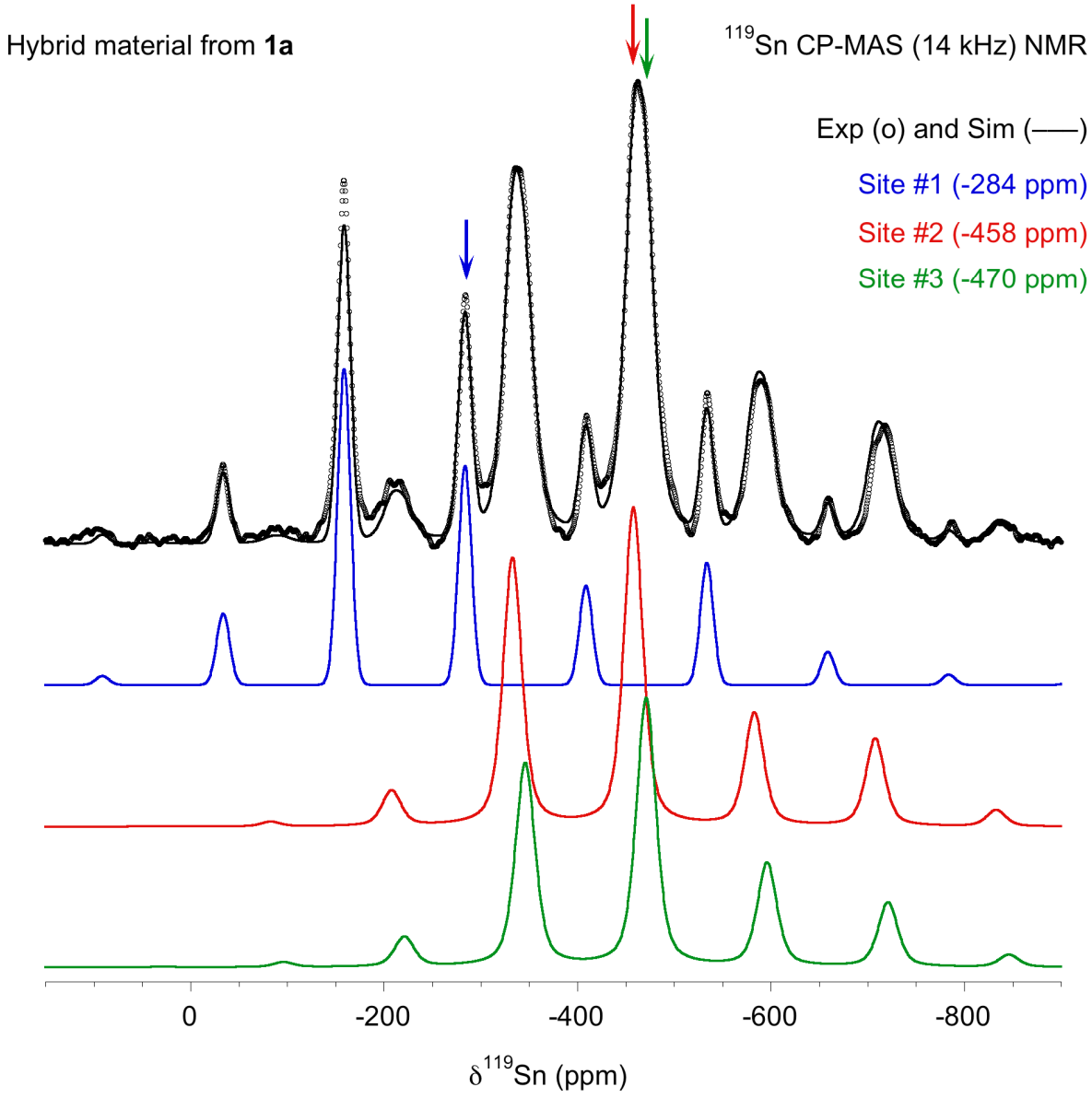

Figure S1A. Experimental and simulated ^{119}Sn CP-MAS spectrum at 14 kHz of the hybrid material prepared from **1a**.

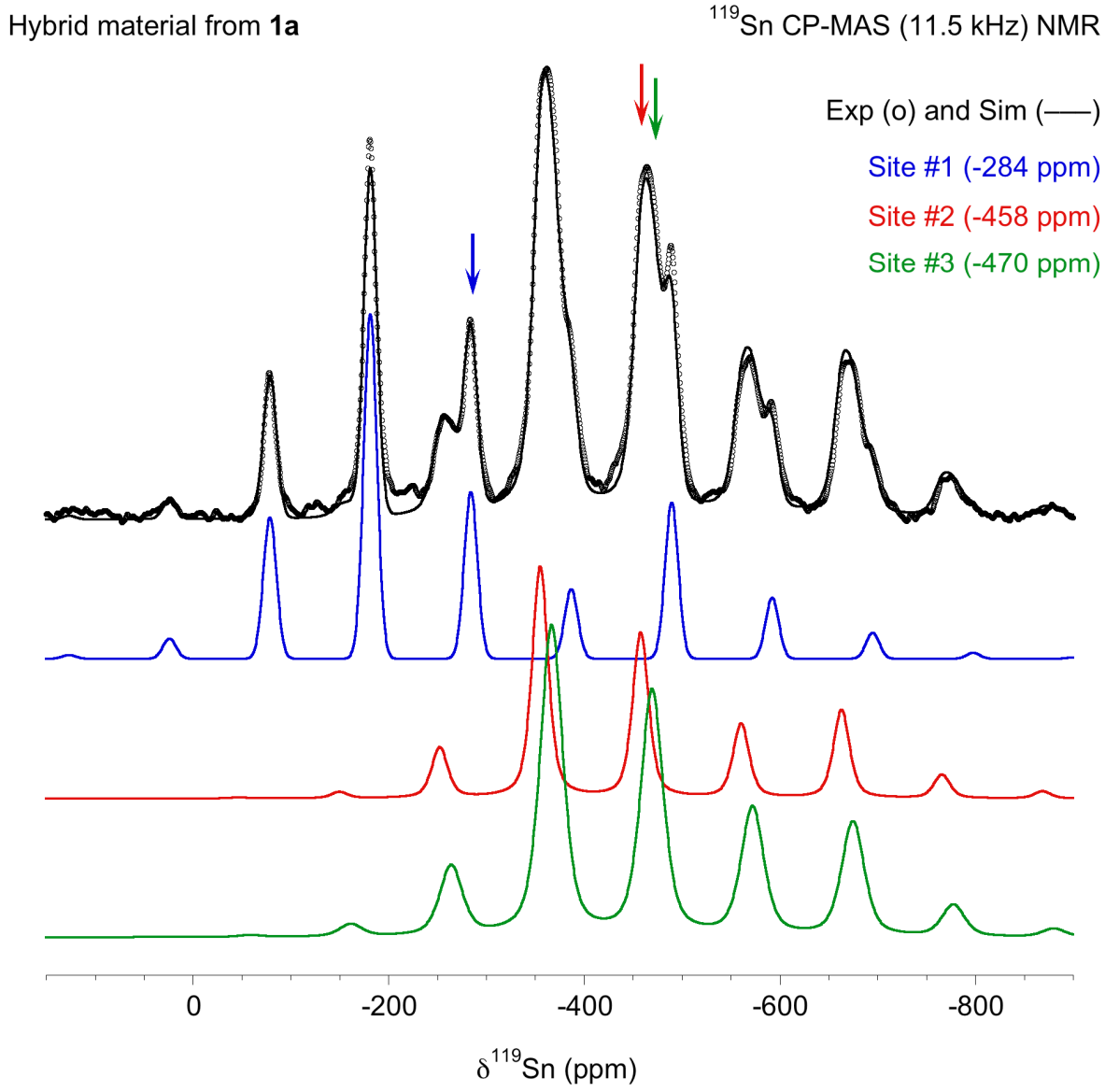

Figure S1B. Experimental and simulated ^{119}Sn CP-MAS spectrum at 11.5 kHz of the hybrid material prepared from **1a**.

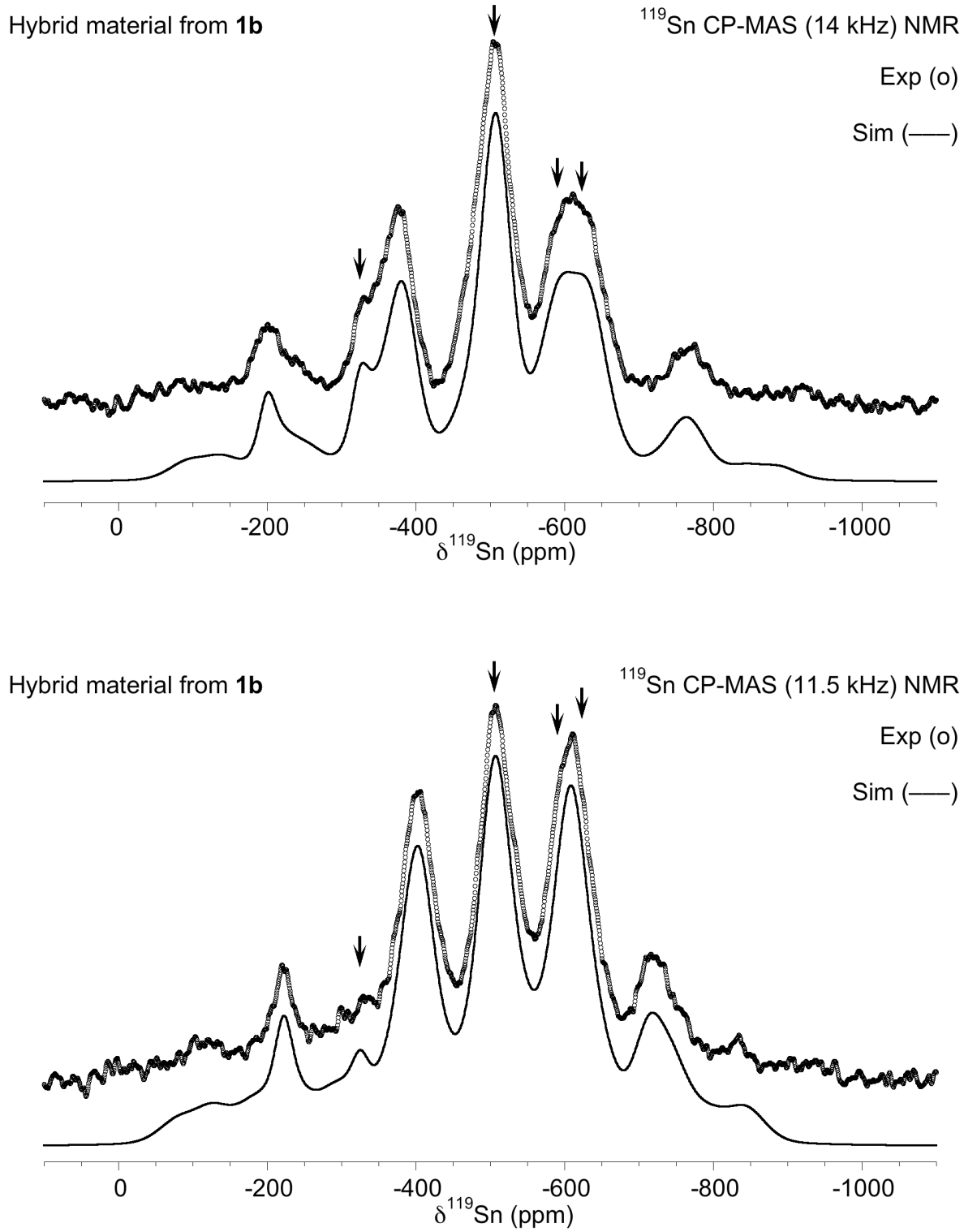

Figure S2. Experimental and simulated ^{119}Sn CP-MAS spectra at 14 kHz (top) and 11.5 kHz (bottom) of the hybrid material prepared from **1b**.

Film preparation

Glass substrates (2cm x 2cm) were washed in refluxing $CHCl_3$ (analytical grade, Aldrich) for 15 min. Then, they were exposed to UV-ozone (home-made apparatus, λ = 254 nm) for 30 min on each side. In a typical experiment, a mixture of water (0.21 g, 11 mmoles), HCl 1N (0.021 g) and THF (2 g) was added to precursors **1** (0.15 mmole) in THF (2g). The resulting solution (5 drops) was immediately spin-coated (8000 round/min/s then 1000 round/min) for 10 s. After drying in air for 15 min, the layers were annealed at 120°C for 1 (**1a**) or 4h (**1b**) to achieve the hydrolysis-condensation process as evidenced by the disappearance of the 2169 cm^{-1} band assigned to the triple bond stretching vibration of the propynyl group (FTIR).

Film characterization

Infrared spectra were recorded in the absorption mode using a FTIR Perkin-Elmer spectrophotometer. Contact angles were determined on a Krüss DAS 100 apparatus (Drop Shape System DAS 10 Mk2) at room temperature in static mode. The results correspond to the average value of at least three measurements. The values of the polar (γ_S^p) and dispersive (γ_S^d) components of the surface energy (γ_S) were calculated according to the Owens-Wendt theory using the contact angles determined for diiodomethane, ethylene glycol and water.[6] The surface morphology of the films was studied by scanning electron microscopy (SEM) with a JEOL JSM-6700F microscope. AFM images were recorded in the tapping-mode phase imaging using a standard silicon cantilever ($\approx$ 20 N/m) on a commercial ICON AFM (DI-Veeco). XRD investigations were performed by a Seifert PTS 3003 using a Cu anode, an X-ray mirror, a long soller slit and a secondary monochromator.

Sensor tests

To investigate the sensing characteristics of the hybrids, they were processed as thin films without addition of any binder or activation layers as well as without thermal activation on suitable substrates. The dc electrical measurements were performed to monitor the sensor response to H_2 (200, 1000, 10000 ppm) in dry N_2 in absence of oxygen and in O_2 + N_2 mixture (10000 ppm oxygen), and to oxygen (2500, 5000 and 10000 ppm) in dry N_2. The sensor signal (S) is given as the resistance ratio R_0/R_{gas}, where R_{gas} and R_0 denote the sensors' resistances in and without the presence of an analyte gas, respectively.

(6) D.K. Owens, R. C. Wendt, *J. Appl. Sci.,* 1969, **13**, 1741.

Contact angle and surface energy determination

Precursor	θ (deg)	γ_s^d ($mJ.m^{-2}$)	γ_s^p ($mJ.m^{-2}$)	γ_s ($mJ.m^{-2}$)
1a	82.4 ± 0.2	27.7 ± 0.1	5.3 ± 0.1	33.0 ± 0.2
1b	94.3 ± 0.2	24.2 ± 0.2	2.6 ± 0.1	26.8 ± 0.1

Table S1. Contact angle with water (θ) measurements and polar and dispersive components of the surface energy.

Infrared spectrum after the detection of hydrogen

The FTIR spectra of the hybrid films prepared from **1a** and **1b** after gas sensing tests are shown in Figure S3.

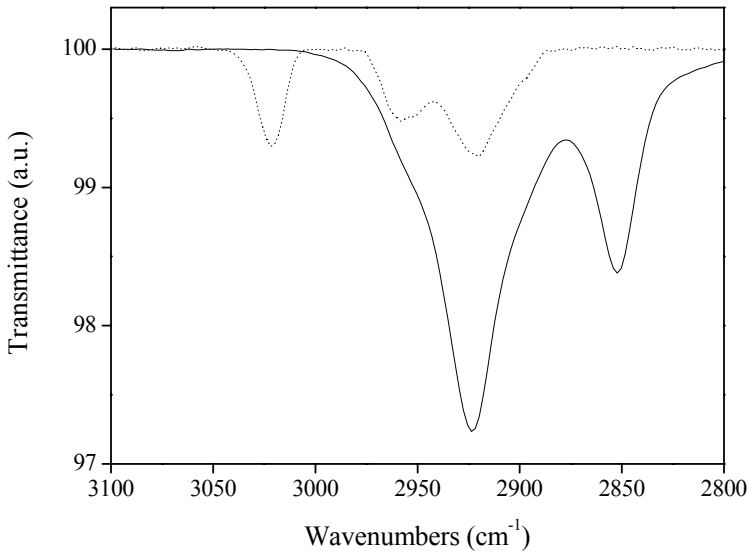

Figure S3. FTIR spectrum (CH stretching vibration region) of the hybrid films prepared from **1a** (full line) and **1b** (dotted line).

Thermogravimetric analysis

Thermogravimetric analyses (Figure S4) of hybrid powders prepared from precursors **1a** and **1b** were recorded between 100 and 650°C under an argon or a nitrogen flow at a heating rate of 10°C/min with a Netzsch STA simultaneous analyzer.

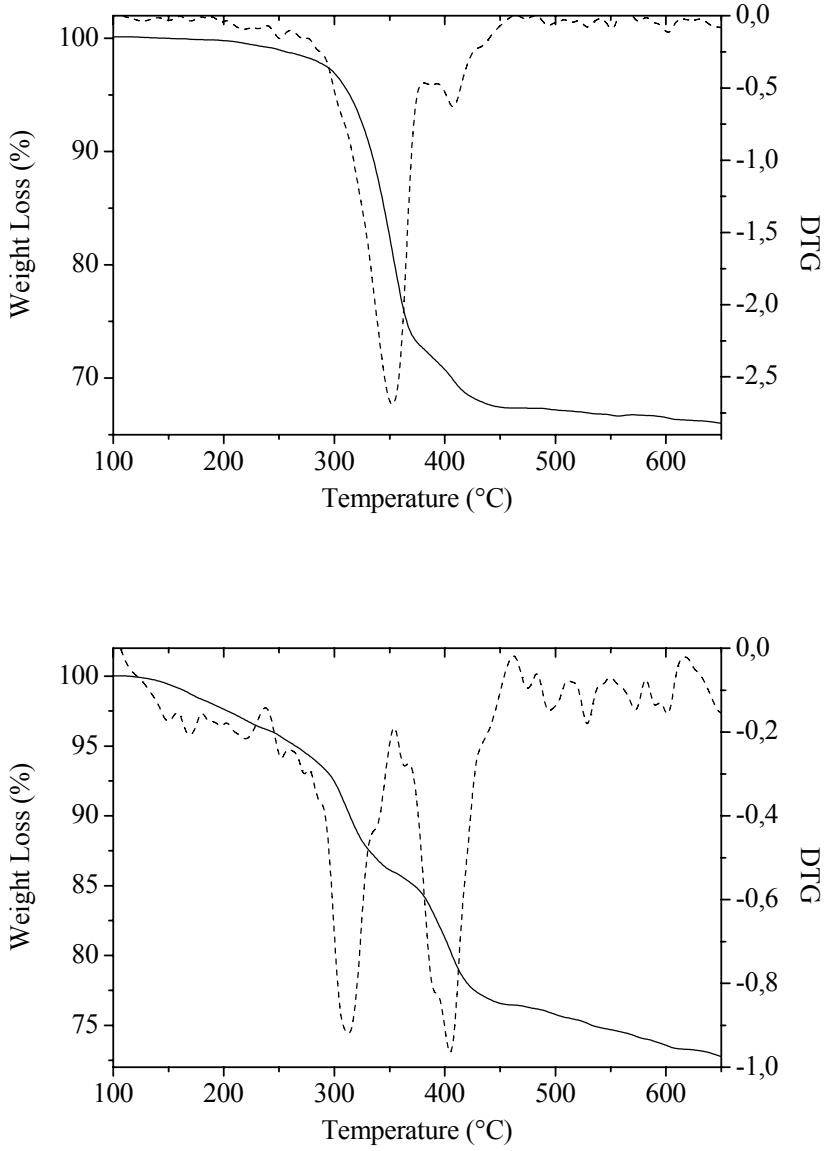

Figure S4. TG and DTG traces of the hybrid powders synthesized from **1a** (top) and **1b** (bottom).

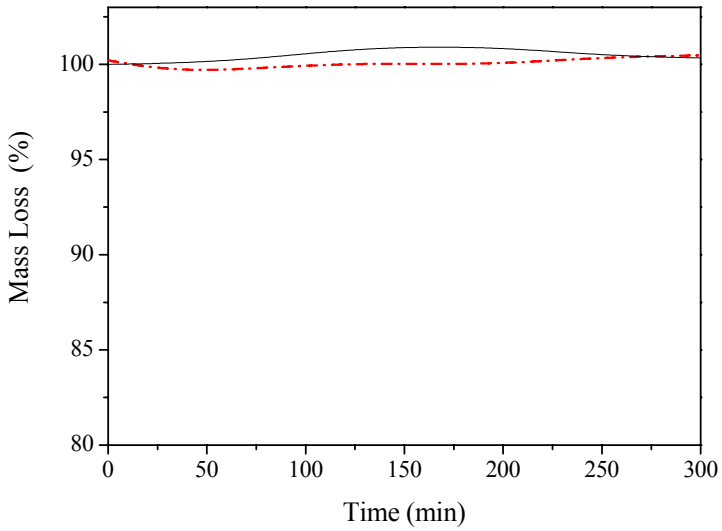

Figure S5. Mass loss as a function of time of the hybrid materials prepared from **1a** (black, full) and **1b** (red, dash) annealed at 200°C under a nitrogen flow.